*Original Research*

# Gene Editing and Small Molecule Inhibitors of the RNA Binding Protein IGF2BP2/IMP2 Show its Potential as an Anti-Cancer Drug Target

Shilpee Chanda[1], Konstantin Lepikhov[2], Charlotte Dahlem[1], Hanna S. Schymik[1], Jessica Hoppstädter[1], An-Kristin Geber[2], Konrad Wagner[3], Sonja M. Kessler[1,4,5], Martin Empting[1,3], Alexandra K. Kiemer[1,6,*]

[1]Department of Pharmacy, Pharmaceutical Biology, Saarland University, 66123 Saarbrücken, Germany
[2]Department of Genetics, Saarland University, 66123 Saarbrücken, Germany
[3]Department of Drug Design and Optimization, Helmholtz Institute for Pharmaceutical Research Saarland (HIPS), Saarland University, 66123 Saarbrücken, Germany
[4]Halle Research Centre for Drug Therapy (HRCDT), 06120 Halle, Germany
[5]Institute of Pharmacy, Experimental Pharmacology for Natural Sciences, Martin Luther University Halle-Wittenberg, 06120 Halle, Germany
[6]Center for Gender-Specific Biology and Medicine (CGBM), 66421 Homburg, Germany
*Correspondence: pharm.bio.kiemer@mx.uni-saarland.de (Alexandra K. Kiemer)
Academic Editor: Milena Georgieva

**Abstract**

**Background**: The RNA-binding protein IGF2BP2/IMP2/VICKZ2/p62 is an oncofetal protein that is overexpressed in several cancer entities. Employing IMP2 knockout colorectal cancer cells, we could show the important role of IMP2 in several hallmarks of cancer. This study aimed to functionally characterize IMP2 in lung (A549, LLC1) and hepatocellular carcinoma (HepG2, Huh7) cell lines to assess its role as a potential target for these cancer entities. **Methods**: IMP2 knockouts were generated by CRISPR/Cas9 and its variant approach prime editing; the editing efficiency of two single guide RNAs (sgRNAs) was verified via next-generation sequencing. We studied the effect of IMP2 knockout on cell proliferation, colony formation, and migration and employed small-molecule inhibitors of IMP2. **Results**: Despite multiple attempts, it was not possible to generate IMP2 biallelic knockouts in A549 and Huh7 cells. Both sgRNAs showed good editing efficiency. However, edited cells lost their ability to proliferate. The attempt to generate an IMP2 biallelic knockout in LLC1 cells using CRISPR/Cas9 was successful. Monoallelic knockout cell lines of IMP2 showed a reduction in 2D cell proliferation and reduced migration. In 3D cultures, a change in morphology from compact spheroids to loose aggregates and a distinct reduction in the colony formation ability of the IMP2 knockouts was observed, an effect that was mimicked by previously identified IMP2 inhibitor compounds that also showed an inhibitory effect on colony formation. **Conclusions**: Our *in vitro* target validation supports that IMP2 is essential for tumor cell proliferation, migration, and colony formation in several cancer entities.

**Keywords:** RNA binding protein; IGF2BP2/IMP2; CRISPR/Cas9; hallmarks of cancer; cell proliferation; colony formation; cell migration; live cell imaging

## 1. Introduction

RNA-binding proteins (RBPs) play an essential role in several cellular functions related to the maturation, stabilization, and localization of mRNAs, as well as the translation of mRNA targets [1]. Insulin-like growth factor 2 (IGF2) mRNA binding proteins (IGF2BPs/IMPs/VICKZs) are oncofetal RBPs overexpressed in several cancers [2], such as lung [3,4], colorectal [5], and liver cancer [6,7]. The term IMP2 denotes the protein form, while *IGF2BP2* and *Igf2bp2* refer to the human and murine gene expression, respectively.

High *IGF2BP2* expression is associated with reduced patient survival and poor prognosis in colon [8–11], liver [10,12], and lung carcinomas [3]. Several studies have suggested a crucial role of IMP2 in promoting tumor cell

hallmarks, such as cell proliferation, colony formation, and migration, in cancer [9,13–15]. These studies utilized siRNA-mediated knockdown of *IGF2BP2*. However, siRNA only provides temporary gene silencing at the mRNA level and might exert distinct unspecific effects [16], while CRISPR/Cas9 enables complete and permanent silencing at the DNA level, inducing mutations that result in protein knockout [17]. CRISPR/Cas9-generated single-cell clones are valuable for investigating protein function, gene loss consequences, and target specificity of potential compounds [18].

Biallelic and monoallelic IMP2 knockout has been achieved in both the CRISPR/Cas9-prime editing-based approach in HCT116 colorectal cancer cells [10]. Small molecule IMP2 inhibitors were identified previously and showed target-dependent effects in wild-type and knock-
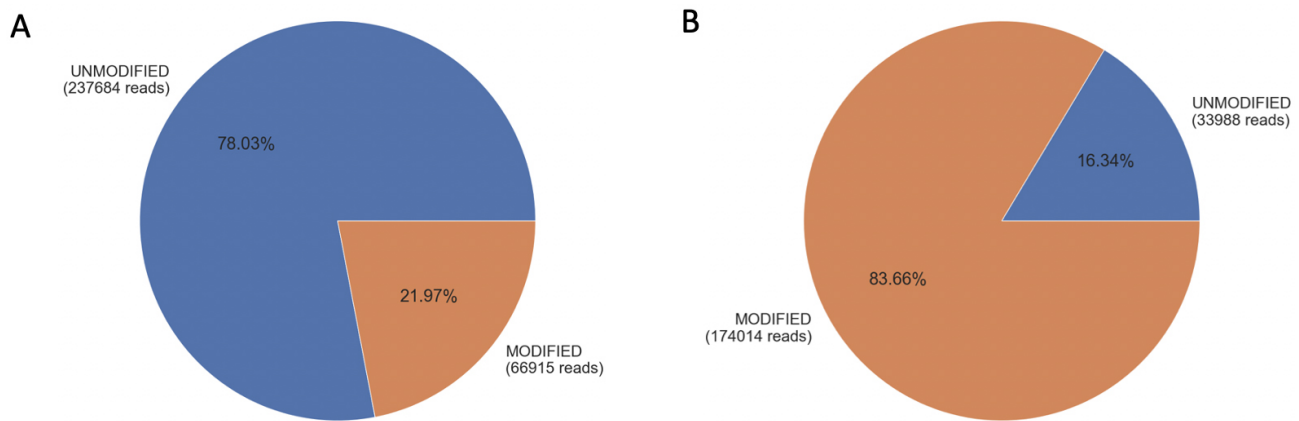
**Fig. 1. Editing efficiency of gRNA1 and gRNA2 in A549 cells.** Panel (A) represents gRNA1-transfected A549 cells analyzed using gRNA1 adapter primers, while panel (B) represents gRNA2-transfected A459 cells using gRNA2 adapter primers. The pie charts display the percentage and number of reads, indicating the presence of unmodified alleles (blue) and modified alleles (orange).

out cells [10]. In this paper, by employing gene editing and small molecule inhibitors, we could verify IMP2 as a tumor-promoting protein in liver, colon, and lung cancer entities.

## 2. Materials and Methods

Complete protease inhibitor cocktail tablets (#04693124001, Roche, Mannheim, Germany), primers, and gRNAs were ordered from Eurofins Genomics, Ebersberg, Germany. SW480 (human, male, colon cancer), and HepG2 (human, male, liver cancer) cells were maintained in Dulbecco's modified Eagle's medium (DMEM, #21969-035, Gibco™, Darmstadt, Germany), and Huh7 (human, male, liver cancer), A549 (human, male, lung cancer), and LLC1 (C57BL mouse, male, primary Lewis lung carcinoma) cells were maintained in Roswell Park Memorial Institute (RPMI-1640 medium, #R0883, Sigma Aldrich, Taufkirchen, Germany). The media were supplemented with 10% fetal calf serum (FCS, #P30-3306, PAN-Biotech, Aidenbach, Germany), 1 mM glutamine (#X0551-100, Biowest, Nuaillé, France), 100 U/mL penicillin, and 100 μg/mL streptomycin (#15070- 063, Gibco™, Darmstadt, Germany). Cell lines were obtained from ATCC. The validation of all cell lines was performed through Short Tandem Repeat (STR) profiling conducted by the Cell Line Authentication Service at Eurofins Genomics in Ebersberg, Germany. PCR-mediated mycoplasma testing was performed regularly. Cells were cultured at 37 °C and 5% $CO_2$. Monoallelic IMP2 knockout Huh7, HepG2, and SW480 cells used in this study were previously generated by ribonucleoprotein delivery mediated CRISPR/Cas9 approach, and the IMP2 inhibitor compounds # 4, 6, and 9 were employed as described earlier [10].

### 2.1 Prime Editing-Mediated IMP2 Knockout

The prime editor 2 system was used to achieve IMP2 knockout in A549, Huh7, and LLC1 cells. pCMV-PE2-P2A-GFP (Addgene plasmid #132776) and pU6- pegRNA-GG-acceptor (Addgene plasmid #132777) were a gift from Anzalone *et al*. [19]. pU6- pegRNA-GG-acceptor plasmid was employed as a vector to deliver the pegRNA component and the designed pegRNA encoding sequences were inserted into the vector by golden gate cloning. A previously validated spacer targeting exon 6 in *IGF2BP2* was used [10], and two different spacers targeting different loci of exon 6 in *Igf2bp2* were utilized for pegRNA assembly (Table 1, Ref. [10]). Desired mutations were planned to disrupt the protospacer adjacent motif (PAM) of the spacer sequences. The scaffold sequence used was:

5′AGAGCTAGAAATAGCAAGTTAAAATAAGGCTA GTCCGTTATCAACTTGAAAAAGTGGCACCGAGTC G-3′ for all pegRNAs.

The knockout procedure: 100,000 cells/well were seeded into 24-well plates and cultivated overnight (16–24 hours). The transfection was initiated when confluence reached approximately 60%. Lipofectamine 3000 (#L3000008, Thermo Fisher Scientific, Darmstadt, Germany) was used for transfection, and an equimolar ratio of the two vectors was employed to obtain a total DNA content of 2 μg, along with lipofectamine reagent in volumes as recommended by the manufacturer. For Huh7 cells, jet-PEI hepatocyte DNA transfection reagent ((#101000053, Polyplus, Illkirch, France) was used according to the manufacturer's instructions. Based on previous trials, media was changed 4 h post-transfection to prevent toxicity associated with the transfection reagents; 24 h post-transfection, cells were gently washed with 1× PBS, followed by detachment using trypsin (#T3924, Merck, Taufkirchen, Germany). The cells were resuspended in media to obtain a single-cell suspension. Single GFP-positive cells were
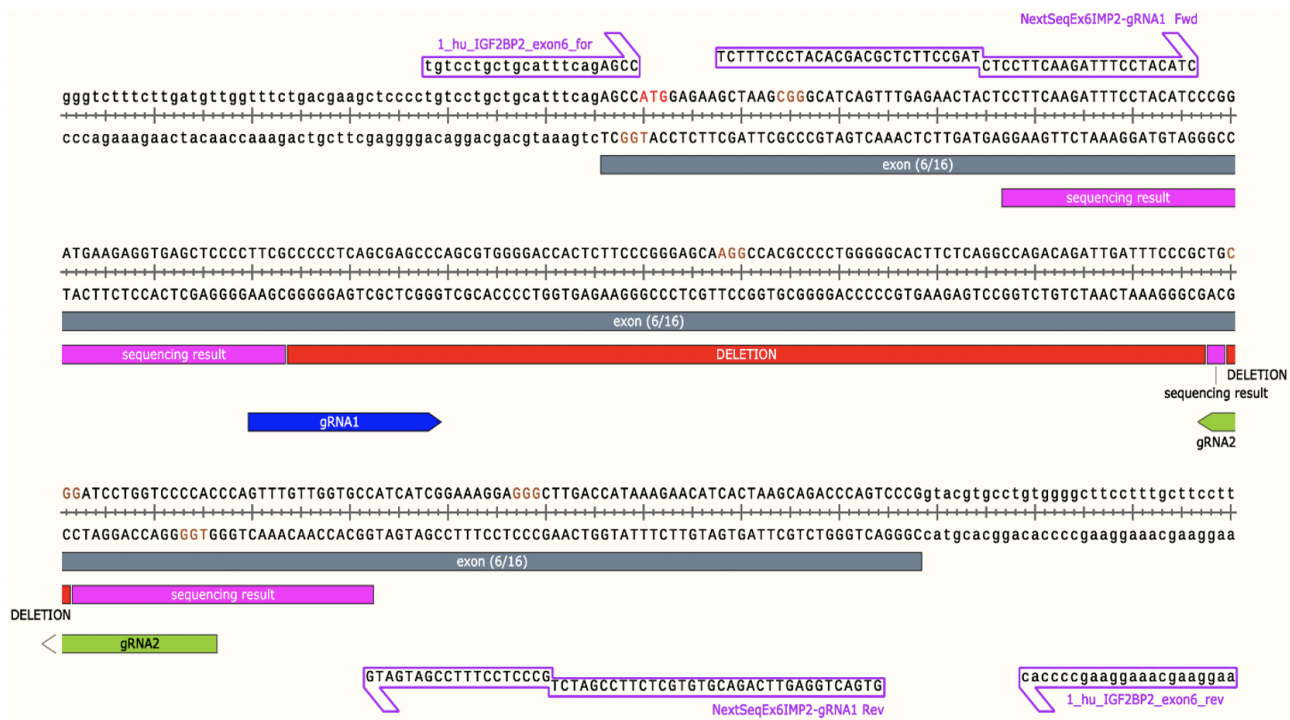
**Fig. 2. Editing efficiency of gRNA1 and gRNA2 in combination in Huh7 cells.** The sequence alignment with the reference genome is presented in the sequence view. Nucleotides indicated by the pink bar represent the sequencing result. Additionally, the red bar represents a 96 bp deletion between the gRNA1 and gRNA2, represented by blue and green bars, respectively. This deletion occurs in the target region of exon 6 of *IGF2BP2*. The image was generated using SnapGene Viewer version 6.2 (San Diego, CA, USA).

**Table 1. Sequences of the components for the assembly of pegRNAs used for IMP2 knockout in human and murine cells using the prime editing approach.**

| Gene name | pegRNA abbreviation | sgSpacer (5′-3′) | pegRNA 3′extension (5′-3′) | PBS length | RTT length |
|---|---|---|---|---|---|
| *IGF2BP2* | pegRNA4_16 | AGAGCCATGGAGAAGCTAAG | TCAAACTGATGCGCTTAGCTTCTCCATGG | 13 | 16 |
| *Igf2bp2* | pegRNA1 | GAGAGCTCACCTCTTCATCG | AAGATTTCCTACATCCGATGAAGAGGTGAGCTC | 15 | 18 |
| | pegRNA2 | GATGATGGCACCAACAAACT | GATCCTGGTCCCCACAGTTTGTTGGTGCCA | 12 | 18 |

Note: pegRNA4_-GG_16ntRT (pegRNA4_16) was validated as described previously [10].

*IGF2BP2*, Insulin-like growth factor 2 (IGF2) mRNA binding protein-2; PBS, Primer-binding site; RTT, Reverse transcription template.

manually picked using a glass capillary and transferred into a petri dish, ensuring enough space between the picked cells so that the resulting colonies would not overlap. A sterile-filtered 48 h conditioned medium from wild-type cells, supplemented with 20% FCS, was utilized to support the growth of the clones. Once the clones reached a sufficient growth point, they were then transferred into a 96-well plate and subsequently cultured in a 24-well plate. They were maintained in culture until the knockout of IMP2 was verified by Sanger sequencing using CRISP-ID to analyze the sequencing results [20], followed by western blot analysis.

### 2.2 CRISPR/Cas9 Mediated IMP2 Knockout

Design of CRISPR/Cas9 system: The CRISPR/Cas9 system was utilized to achieve IMP2 knockout in A549,

Huh7, and LLC1 cells. Here, pSpCas9(BB)-2A-GFP (PX458, Addgene plasmid #48138) plasmid construct was used. Cas9-GFP fusion protein expression cassette was combined with U6-promotor driven sgRNA expression in the single plasmid. Restriction enzyme cloning was employed to insert designed gRNA sequences into the PX458 plasmid construct. Two different gRNAs, namely gRNA1 and gRNA2, were used to target *IGF2BP2*, while gRNAI and gRNAII were used for editing in *Ifg2bp2* (Table 2). The knockout cell lines generation, selection, and isolation procedures were as described in 2.1; however, the total DNA used for transfection was 1 µg.

### 2.3 Next-Generation Sequencing (NGS)

The transfection of the cells was performed as described in section 2.2. After 24 h of transfection, the cells

**Table 2. The gRNA sequences for IMP2 knockout in human and murine cells by CRISPR/Cas9 approach.**

| Name | Sequence (5′-3′) | Target region of *IGF2BP2* |
|---|---|---|
| *IGF2BP2* gRNA1 | GGGCTCGCTGAGGGGGCGAA | Exon 6 |
| *IGF2BP2* gRNA2 | GTGGGGACCAGGATCCGCAG | Exon 6 |
| *Igf2bp2* gRNAI | GAGAGCTCACCTCTTCATCG | Exon 6 |
| *Igf2bp2* gRNAII | GATGATGGCACCAACAAACT | Exon 6 |

gRNA, guide RNA.

**Table 3. Next-generation sequencing adapter primers.**

| Name | Primers | Sequence (5′-3′) |
|---|---|---|
| gRNA1 adapter pair | gRNA1 Fwd | TCTTTCCCTACACGACGCTCTTCCGATCTCCTTCAAGATTTCCTACATC |
| | gRNA1 Rev | GTGACTGGAGTTCAGACGTGTGCTCTTCCGATCTGCCCTCCTTTCCGATGATG |
| gRNA2 adapter pair | gRNA2 Fwd | TCTTTCCCTACACGACGCTCTTCCGATCTGCCCTCCTTTCCGATGATG |
| | gRNA2 Rev | GTGACTGGAGTTCAGACGTGTGCTCTTCCGATCTCCTTCAAGATTTCCTACATC |

were washed with $1\times$ PBS, detached with trypsin (#T3924, Merck, Taufkirchen, Germany), and resuspended to obtain a single-cell suspension; 30–40 GFP-positive cells, as mentioned in section 2.1, were manually picked and added to a PCR tube containing 2 µL of lysis buffer (Phire Tissue Direct PCR Kit, #F170S, ThermoFisher Scientific, Darmstadt, Germany). Heat inactivation of Proteinase K in the lysis buffer was performed at 96 °C for 3 min.

Amplification of the specific target region in *IGF2BP2* (Table 2) was carried out by PCR using the following primers: hIMP2 exon 6_for 5′-TGTCCTGCTGCATTTCAGAGCC-3′ and hIMP2 exon 6_rev 5′-AAGGAAGCAAAGGAAGCCCCAC-3′, as described previously [10]. For the first PCR, we used the Phire Tissue Direct PCR Master Mix (F170S, Thermo Scientific, Darmstadt, Germany) following the manufacturer's protocol. The amplified product was purified by agarose gel electrophoresis using the NucleoSpin® Gel and PCR Clean-up kit (#11992242, Macherey-Nagel, Düren, Germany) to obtain the desired size amplicon of 323 bp and to remove PCR residues, such as nucleotides, salt, and primers, that could interfere with the downstream processing.

In the second PCR, the primers bound to NGS-sequencing adapters (Table 3) were used, and the KAPA2G Fast Hot Start Genotyping Mix (KK5620, Sigma Aldrich, Taufkirchen, Germany) was employed following the manufacturer's instructions. The PCR product was subjected to agarose gel purification. Subsequent sequencing was performed on an Illumina NextSeq platform using single-end sequencing. The sequencing results were analyzed using the CRISPResso2 software package [21].

### 2.4 Western Blot

Western blots were performed as described earlier [6], employing antibodies specific for IMP2/p62 [22] and $\alpha$-tubulin (#T9026, Merck, Taufkirchen, Germany). The secondary antibodies used were IRDye680-conjugated anti-rabbit IgG (#926-68071, LI-COR Bioscience, Bad Hom-

burg, Germany) and IRDye800- conjugated anti-mouse IgG (#926-32210, LI-COR Bioscience, Bad Homburg, Germany). The Odyssey near-infrared imaging system from LI-COR Bioscience (Bad Homburg, Germany) was used to measure the signal intensities for IMP2 and its splice variant p62. The quantification of the western blot signal intensities was performed using StudioLite software version 5.0 (LI-COR Bioscience, Bad Homburg, Germany).

### 2.5 Cell Proliferation in 2D

The IncuCyte® S3 system (Sartorius, Goettingen, Germany) was employed to monitor 2D cell proliferation; 3000 cells per 100 µL per well were seeded into a 96-well plate. For compound treatment, solvent control (0.1% DMSO dissolved in respective media) was also tested, and compounds were added to the cell the day after seeding. Cell confluency was measured every 8 h starting from the time point of treatment or seeding (for experiments without compound treatment) until 72 h and analyzed using the basic analyzer software. Cell confluency was normalized to the 0 h time point. Metabolic activity was measured 72 h after seeding using the MTT assay. For each compound, the inhibition of cell viability was calculated for each concentration and normalized to its respective DMSO control or untreated control (if DMSO control showed viability above 90%).

### 2.6 MTT Assay

60,000 cells per 100 µL per well were seeded into a 96-well plate. For compound treatment, solvent control (0.1% DMSO dissolved in respective media) was also tested, and compounds were added to the cells the day after seeding. Metabolic activity was measured 72 h after treatment using the MTT assay. For each compound, the inhibition of cell viability was calculated for each concentration and normalized to its respective DMSO control or untreated control (if DMSO control showed viability above 90%).
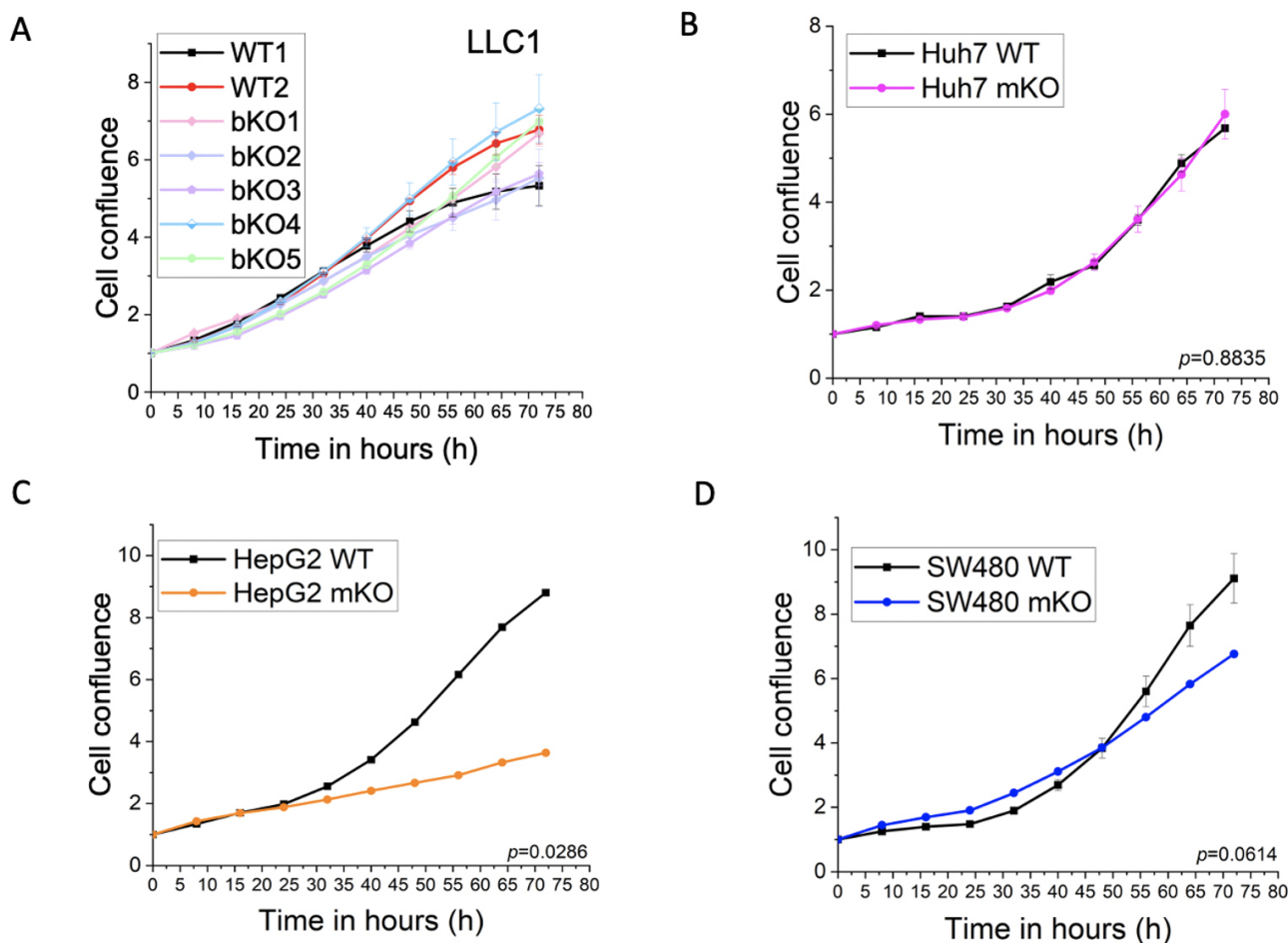
**Fig. 3. Effect of IMP2 knockout on 2D cell proliferation.** (A) LLC1, (B) Huh7, (C) HepG2, and (D) SW480 were assessed for their effect on 2D cell proliferation using the IncuCyte® S3 live cell imaging system. LLC1 IMP2 knockouts were biallelic (bKO), while the Huh7, HepG2, and SW480 cells were monoallelic IMP2 knockouts (mKO). Data were normalized to time point 0 h and are represented as mean ± SEM, n = 3, quintuplicates. Significance values were determined by comparing the knockout cells to those obtained from the wild-type (WT) cells. The proliferation rate was determined based on cell confluence.

### 2.7 Spheroid Formation Assay

To assess the spheroid-forming ability of cells in 3D, the IncuCyt® S3 system was used. 3000 cells per 100 µL per well were seeded into low-attachment U-bottom 96-well plates. Spheroid formation was monitored over 6 days after seeding.

### 2.8 Colony Formation Assay

Using serial dilution, 300 cells per 2 mL per well were seeded into a 6-well plate. For compound treatment, solvent control (0.1% DMSO dissolved in respective media) was also tested, and compounds were added to the well at the time of seeding. Cells were allowed to grow for 1–2 weeks to assess the colony formation ability. The media was removed, and cells were washed once carefully using 1× PBS. The live colonies were imaged using the IncuCyte® S3 system. The confluence area was measured for colonies consisting of at least 50 cells per colony, which corresponded to an object area of at least $1 \times 10^4$–$2 \times 10^4$ µm$^2$, depending on the cell type, and the cut-off mask was applied accordingly. The object counts per well module provided the total count of the colonies per well. The object average area module provided the average colony area per well. The inhibition of colony formation activity was calculated by normalizing to its untreated control (if solvent control did not show any difference in the number and size of colony in comparison to the untreated).

### 2.9 Wound Healing Assay

A total of 70,000 cells were seeded per 100 µL per well into an Image Lock 96-well plate. On the following day, the wound maker tool was used to perform scratches into the cell monolayers. The media containing the detached cells were removed and replaced with media without FCS. Migration was observed every 8 h up to 48 h after scratching. Cell confluency in the wound area was analyzed using IncuCyte® S3 migration software.
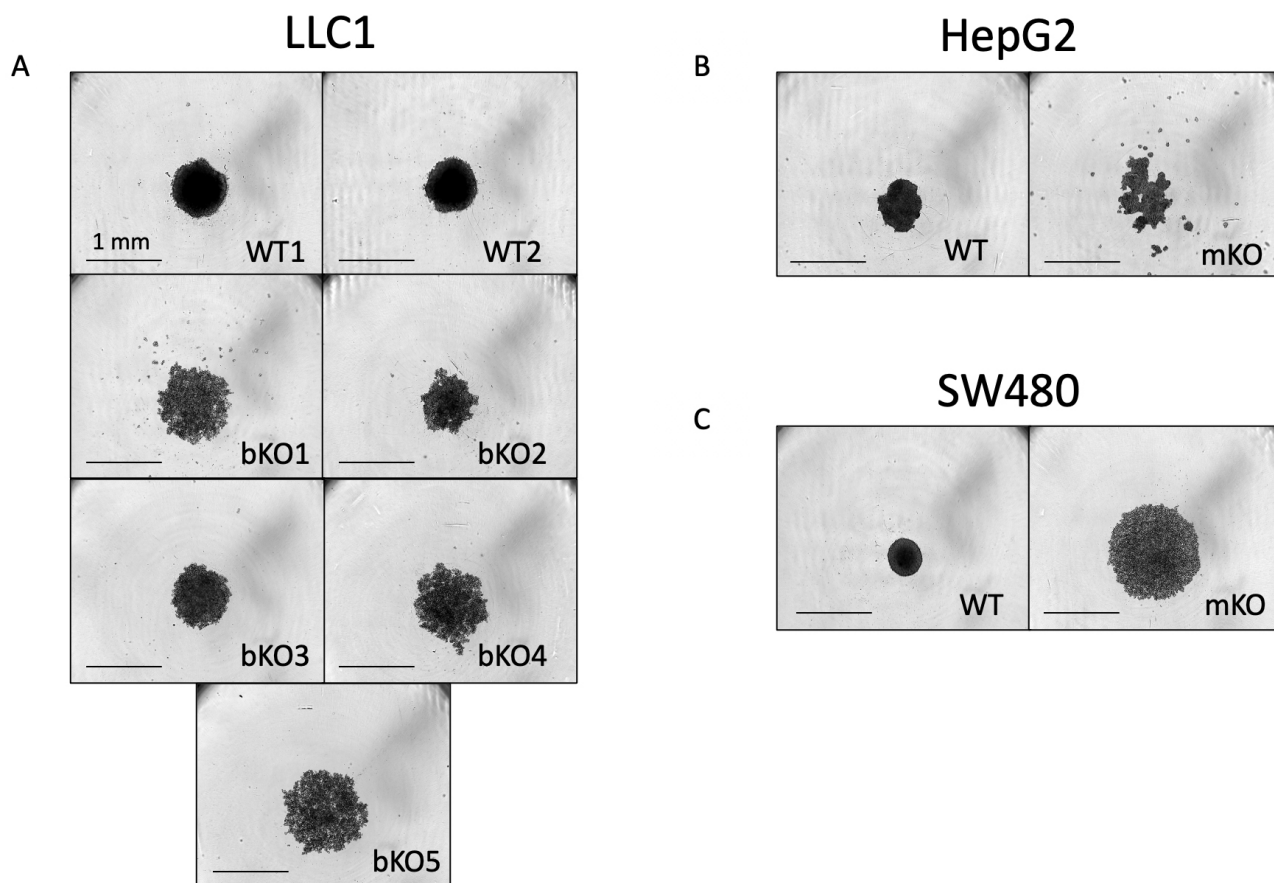
**Fig. 4. Comparison of spheroid formation between wild-type and IMP2 knockout clones.** (A) LLC1, (B) HepG2, and (C) SW480 clones were assessed for their spheroid forming ability using the live cell imaging system IncuCyte® S3 at the 6-day time point after cell seeding. Representative images were chosen, and the scale was adjusted to 1 mm. The Huh7, HepG2, and SW480 IMP2 knockout cells were monoallelic knockouts.

*2.10 Statistical Analysis*

The raw data was analyzed using Microsoft Excel, and statistical analysis was performed using Origin Pro® version 2023b software (Northampton, MA, USA). Non-linear regression analysis was used to calculate the inhibitory concentration 50 ($IC_{50}$). Data are presented as means $\pm$ SEM unless otherwise indicated. To analyze the data distribution, the Shapiro-Wilk test was performed, and subsequent analysis was conducted based on the distribution and group size. Statistical differences between groups were calculated on the group number using Student's *t*-test for two groups and one-way ANOVA with Tukey's or Bonferroni's *post hoc* analysis for more than two groups at a single time point. Statistical differences between groups at several time points were calculated using two-way ANOVA with Bonferroni's post hoc analysis. $*p < 0.05$, $**p < 0.01$, $***p < 0.001$.

# 3. Results

*3.1 Prime Editing, a CRISPR/Cas9 Variant Method, could not Achieve IMP2 Knockout Cells*

Prime editing, a CRISPR/Cas9 variant, had previously achieved biallelic IMP2 HCT116 knockout cells [10]. However, despite multiple trials, IMP2 knockout generation using this approach (Table 1) in HepG2, Huh7, SW480, A549, and LLC1 cells was not successful.

*3.2 NGS Confirms the Editing Efficiency of RNAs Employed in the CRISPR/Cas9 Approach*

Multiple attempts to generate IMP2 knockouts in A549 and Huh7 cells using the CRISPR/Cas9 approach also failed. To rule out any effect of the manual single-cell picking procedure and further culture, we applied the entire single-cell colony expansion procedure on non-transfected A549 and Huh7 cells. While both non-transfected and GFP-negative cells, which had undergone the same transfection technique, formed colonies, no edited clones in either cell line were obtained.

To test the hypothesis that the inability of the successfully edited single cells to proliferate into a colony was since
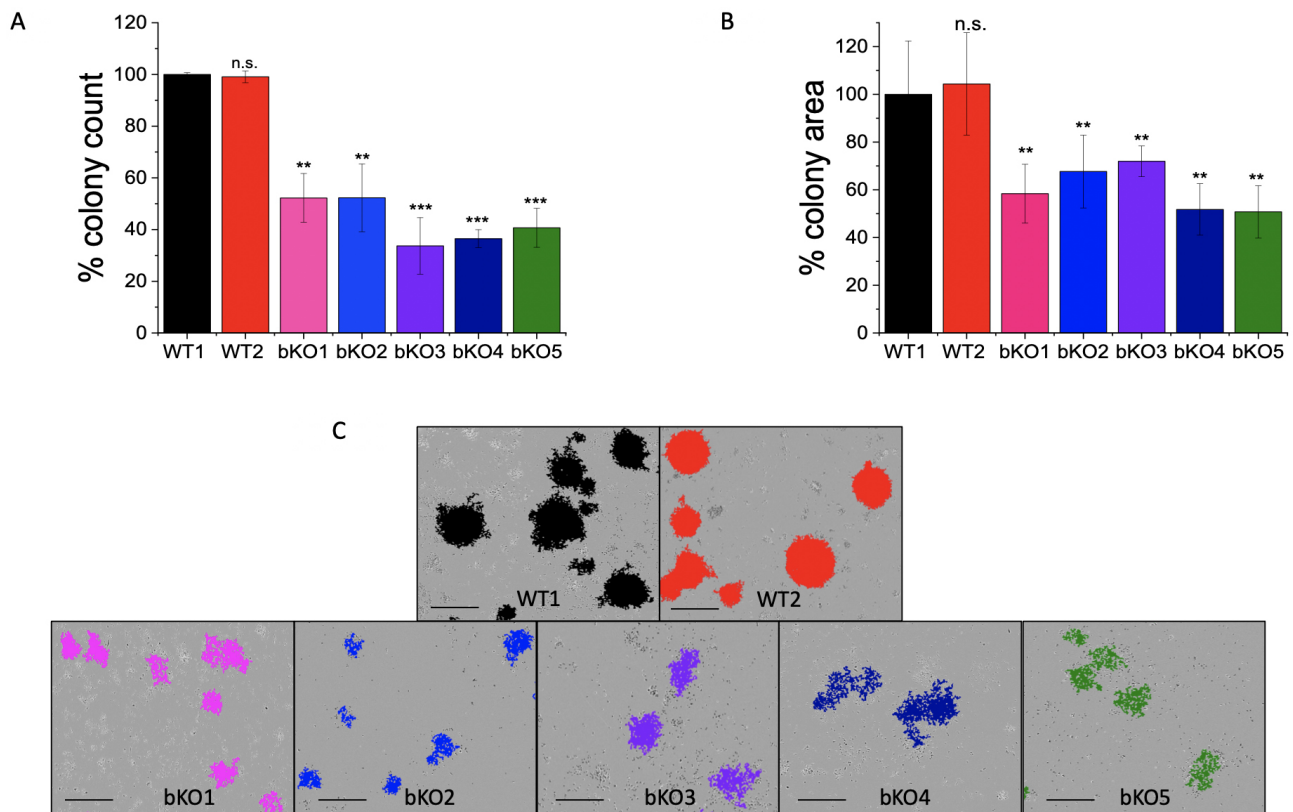
**Fig. 5. Effect of IMP2 knockout in LLC1 cells on the colony formation ability.** The results are presented as follows: (A) number of colonies, (B) average area of colonies, and (C) representative images of colonies with the scale adjusted to 1 mm. Colony counting and measurement of average area were performed using the IncuCyte® S3 live cell imaging system. It should be noted that WT1 represents the LLC1 wild-type clone, while WT2 serves as the LLC1 editing control. The data was normalized to the WT1 cells and are represented as mean $\pm$ SEM, n = 4, triplicates. **$p < 0.01$ and ***$p < 0.001$ when compared to values of WT1 cells. n.s. indicates no significant difference.

IMP2 is necessary for cell survival and proliferation, we performed next-generation sequencing of the GFP-positive cells picked up 24 h post-transfection that were successfully transfected with gRNA1 or gRNA2 individually in A549 cells or combination in Huh7 cells. Furthermore, as a control for the next-generation sequencing method, we simultaneously analyzed a separate batch of A549 and Huh7 cells that were not transfected at all. These cells are referred to as the non-transfected cells.

The sequencing analysis of GFP-positive A549 cells transfected with gRNA1 revealed a modification of 21.97% (Fig. 1A), while transfection with gRNA2 exhibited a higher editing efficiency of 83.66% (Fig. 1B). Similarly, GFP-positive Huh7 cells transfected with gRNA1 showed a comparable editing efficiency (**Supplementary Fig. 1D**), providing further evidence that gRNA editing efficiency is independent of the cell line.

In the case of non-transfected A549 cells, the analysis using gRNA1 and gRNA2 adapter primers showed that 99% (**Supplementary Fig. 1A**) and 98.9% (**Supplementary Fig. 1B**) of the alleles matched the reference sequence near the gRNA target site, respectively. Sim-

ilar results were observed for non-transfected Huh7 cells analyzed using gRNA1 adapter primers (**Supplementary Fig. 1C**). It is important to note that the modifications depicted in Fig. 1 and **Supplementary Fig. 1** include base insertions, deletions, and substitutions.

The next-generation sequencing analysis of Huh7 cells transfected with both gRNA1 and gRNA2 revealed a deletion of 96 base pairs between the expected cut sites of the two sgRNAs, as determined using the gRNA1 adapter primer system (Fig. 2). This finding provides additional evidence supporting the high editing efficiency of gRNA1 and gRNA2.

### 3.3 CRISPR/Cas9-Facilitated Igf2bp2 Knockout in LLC1 Cells

IMP2 biallelic knockout LLC1 cells were generated using gRNAI and gRNAII (Table 2). The editing was confirmed through Sanger sequencing analysis, and six different mutation types were observed (**Supplementary Fig. 2**). A representative clone of each mutation type was selected for further investigation. The reduction in IMP2 expression was confirmed through western blot analysis
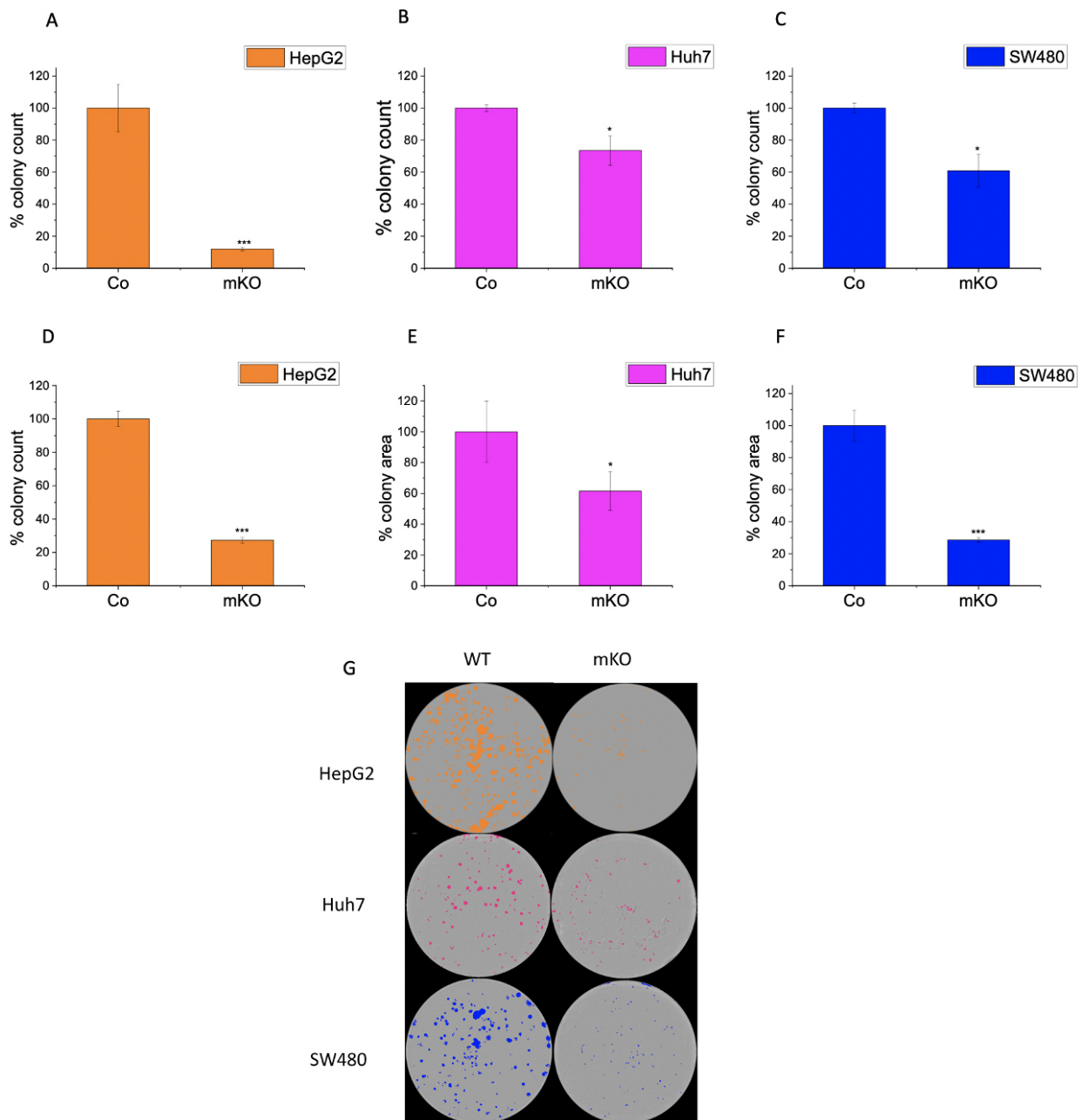
**Fig. 6. Effect of IMP2 knockout on colony formation ability of Huh7, HepG2, and SW480.** Figures illustrate the number of colonies for wild-type (WT) or monoallelic IMP2 knockout (mKO) (A) Huh7, (B) HepG2, and (C) SW480 cells, and the average area of colonies for (D) Huh7, (E) HepG2, and (F) SW480. (G) Representative images of colonies seen in a 6-well plate. The colonies were counted, and the average colony area was measured using the IncuCyte® S3 live cell imaging system. Huh7, HepG2, and SW480 were monoallelic IMP2 knockouts. Data were normalized to wild-type cells/control (Co) and represented as mean $\pm$ SEM, n = 3, duplicates. *$p < 0.05$ and ***$p < 0.001$ when compared to values of control.

(**Supplementary Fig. 3**). However, the clone bKO6 exhibited up to 65% expression of IMP2 compared to LLC1 wild-types (WT1) and was therefore excluded from further analysis. The remaining five clones, designated as bKO1, bKO2, bKO3, bKO4, and bKO5, were utilized for subsequent characterization. To assess the potential off-target effects of the CRISPR/Cas9-mediated knockout procedure,

an editing control LLC1 clone named WT2 was included in the experimental analysis. This control clone was obtained from an experiment in which cells had undergone transfection with both gRNAI and gRNAII but were selected from non-GFP positive cells. Sanger sequencing confirmed that WT2 was a wild-type clone.
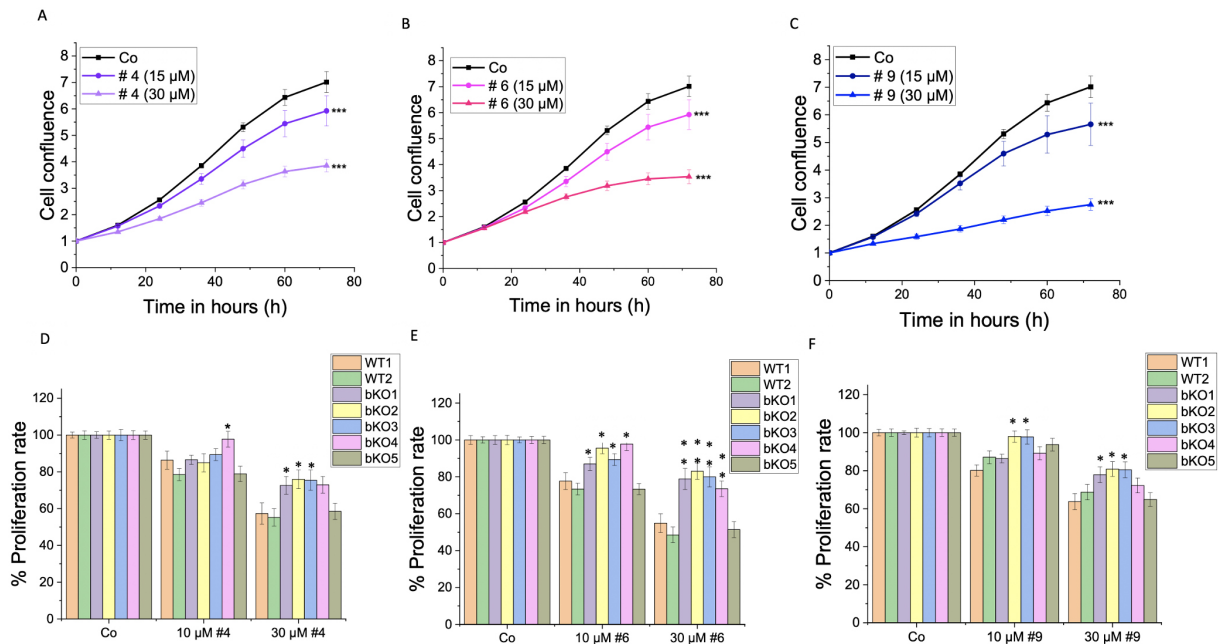
**Fig. 7. Effect of IMP2 inhibitors on the 2D cell proliferation of wild-type and biallelic IMP2 knockout LLC1 cells.** The effects on 2D proliferation of LLC1 cells upon treatment with published IMP2 inhibitors, i.e., (A,D) compound 4, (B,E) compound 6, and (C,F) compound 9 at the indicated concentrations over 3 days were assessed using the IncuCyte® S3 live cell imaging system. The time point shown in panels (D–F) is 72 h post-treatment. Data is normalized to time point 0 h of the respective control and represented as mean ± SEM, n = 3, triplicates. *$p < 0.05$, **$p < 0.01$, and ***$p < 0.001$ when compared to values of control (Co) for graphs (A–C) and to the values of WT1 LLC1 cells for graphs (D–F). The proliferation rate was determined based on the cell confluence.
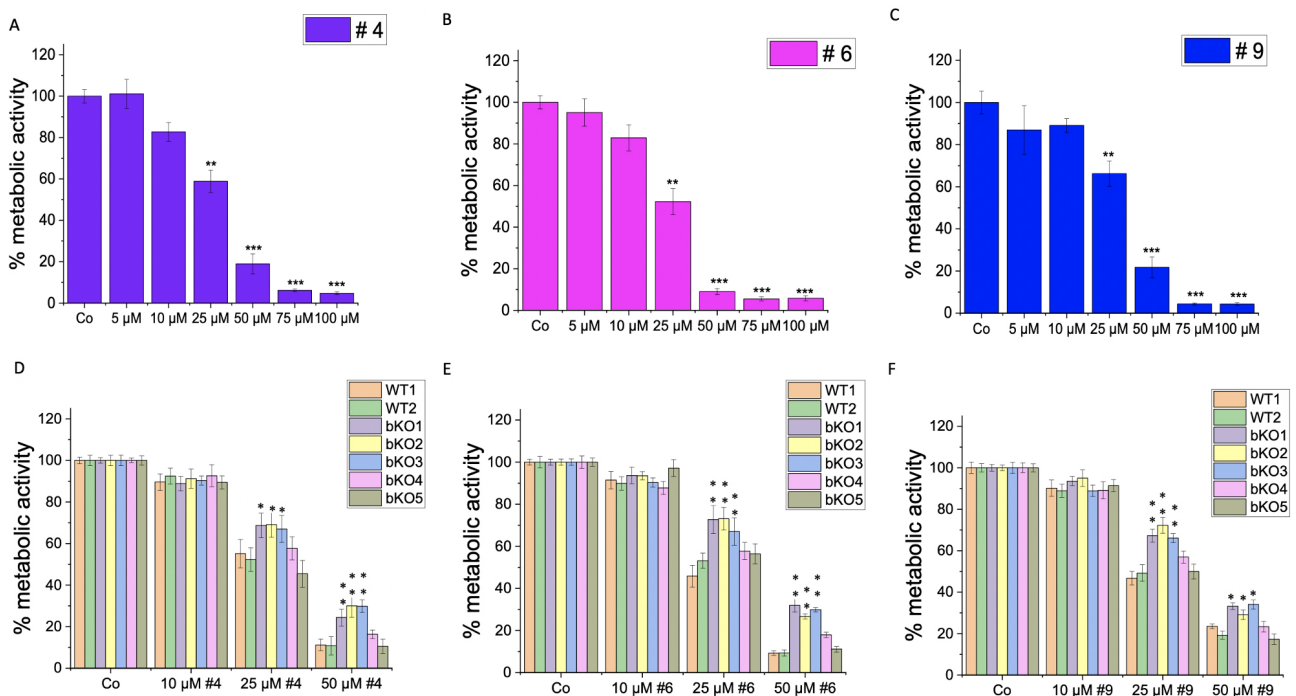


**Fig. 8. Effect of IMP2 inhibitors on the metabolic activity (MTT assay) of wild-type and biallelic IMP2 knockout LLC1 cells.** The effects on the metabolic activity of LLC1 cells upon treatment with published IMP2 inhibitors, i.e., (A,D) compound 4, (B,E) compound 6, and (C,F) compound 9 at the indicated concentrations after 3 days were assessed by MTT assay. Data are normalized to solvent controls (Co) and represented as mean ± SEM, n = 3, triplicates. *$p < 0.05$, **$p < 0.01$, and ***$p < 0.001$ when compared to values of control (Co) for graphs (A–C) and to the values of WT1 LLC1 cells for graphs (D–F).

*3.4 In Vitro IMP2 Target Validation*

To conduct the *in vitro* IMP2 target analysis, biallelic knockout clones were utilized where available. However, for cell lines in which achieving a biallelic knockout (bKO) was not possible, monoallelic knockout (mKO) clones were employed. The IMP2 protein levels in the monoallelic knockouts have been previously published. The mean values were close to 80% for Huh7, 44% for HepG2, and 57% for SW480 [10], while the expression of IMP2 in the biallelic LLC1 knockouts is shown in **Supplementary Fig. 3.**

### 3.4.1 IMP2 Knockout Reduces Proliferation in 2D Cell Culture

Compared to the WT2 control, which had undergone the same treatment as the knockout clones, clones bKO1-3 showed reduced proliferation (bKO1: $p = 0.037$; bKO2: $p = 0.005$; bKO3: $p < 0.0001$). However, the growth rate of the two wild-type controls varied quite strongly (Fig. 3A). No apparent morphological changes were observed in the wild-type and biallelic IMP2 knockout LLC1 cells (**Supplementary Fig. 4A**).

No effect was seen in the proliferation of the monoallelic knockout clones of Huh7 (Fig. 3B). Although not statistically significant, a trend towards reduced proliferation was observed for the SW480 monoallelic knockout clone at later time points (Fig. 3D). Importantly, a significant reduction in proliferation was observed in the HepG2 IMP2 knockout clone (Fig. 3C).

### 3.4.2 IMP2 Knockout Cells Lose Their Ability to Form Compact 3D Spheroids

3D cell culture models, also known as multicellular tumors (MCTs) or spheroids, closely resemble the structural organization, oxygen and nutrient gradients, and pH conditions of *in vivo* solid tumors [23]. Based on the compactness, the spheroid/multicellular tumors (MCTs) are categorized as compact spheroids and loose aggregates of cells [23]. Compact spheroids are tightly bound to each other, making it difficult to distinguish single cells, whereas loose spheroids cannot form complete spheres and can be easily disintegrated [23]. In some tumor cell types, they fail to aggregate into one single entity and exist as several small colonies of cells, which are referred to as satellite colonies. We observed a loss in the ability to form compact spheroids upon the knockout of IMP2. All wild-type clones except for Huh7 successfully formed compact spheroids three days after seeding. In contrast, the biallelic IMP2 knockout LLC1 cells and the monoallelic IMP2 knockout SW480 cells showed a change in cell adhesion and formed loose aggregates, while the monoallelic HepG2 IMP2 knockouts formed satellite colonies. This characteristic persisted even after 6 days of observation (Fig. 4). Parental Huh7 cells also showed the formation of satellite colonies and did not form spheroids throughout the 6-day observation period (data not shown).

### 3.4.3 IMP2 Knockout Clones and Treatment of Wild-Type Cells with IMP2 Inhibitors Exhibited Impaired Colony Formation Ability

The colony formation assay (CFA) provides insight into the ability of single cells to survive and reproduce [24] and has been extensively used to test the effect of cytotoxic agents on a cancer cell's ability to form a viable colony [25]. The CFA was employed to understand the role of IMP2 in tumor growth. The LLC1 IMP2 biallelic knockout cells exhibited a significant decrease in both the number of colonies formed (Fig. 5A) and the average area of the colonies (Fig. 5B). While the wild-type cells formed colonies in the form of spheroids, the knockout clones lost this ability (Fig. 5C). Furthermore, monoallelic IMP2 knockouts of Huh7, HepG2, and SW480 cells also exhibited a significant reduction in colony formation ability, as observed in terms of both colony number and area (Fig. 6).

Furthermore, we investigated the impact of IMP2 inhibitor compounds # 4, 6, and 9, which had been identified by a screening approach [10], on the 2D proliferation and metabolic activity of wild-type LLC1 cells. The compounds demonstrated a significant reduction in the proliferation rate at concentrations of 15 μM and 30 μM (Fig. 7A–C), and a dose-dependent decrease in the cells' metabolic activity, as assessed by MTT assay, was observed at concentrations ranging from 5 μM to 100 μM (Fig. 8A–C). The cells did not exhibit distinct morphological changes (**Supplementary Fig. 4B**).

To investigate the specificity of the compounds on IMP2 in terms of their effect on 2D proliferation (Fig. 7D–F) and metabolic activity (Fig. 8D–F), we compared their action on bulk WT1 and the editing control WT2 and the five biallelic IMP2 knockout LLC1 clones. Notably, the knockout clones bKO1-4 displayed a lower sensitivity to the treatments compared to wild-type LLC1 cells (WT1 and WT2). The bKO5 displayed a similar response to the wild-type LLC1 cells.

Based on the $IC_{50}$ of the compounds on LLC1 metabolic acitivity, a treatment concentration of 25 μM was chosen for our study of their effect on colony formation (Table 4). For HepG2, Huh7, and SW480, the previously published $IC_{50}$ values of the three compounds were selected for the treatment [10]. In all tested cell lines, all three compounds exhibited a significant reduction in both the number and average size of the formed colonies. These findings provide further evidence of the essential role of IMP2 in colony formation ability (Figs. 9,10).

### 3.4.4 IMP2 Knockout Cells Show Reduced Cell Migration

The effect of IMP2 knockout on cell migration was investigated (Fig. 11). The two parental LLC1 cell lines, namely WT1 and WT2, differed significantly ($p < 0.0001$), with the WT2 migrating slower than the bulk WT1 cells. The IMP2 biallelic LLC1 knockout cells were heterogenous
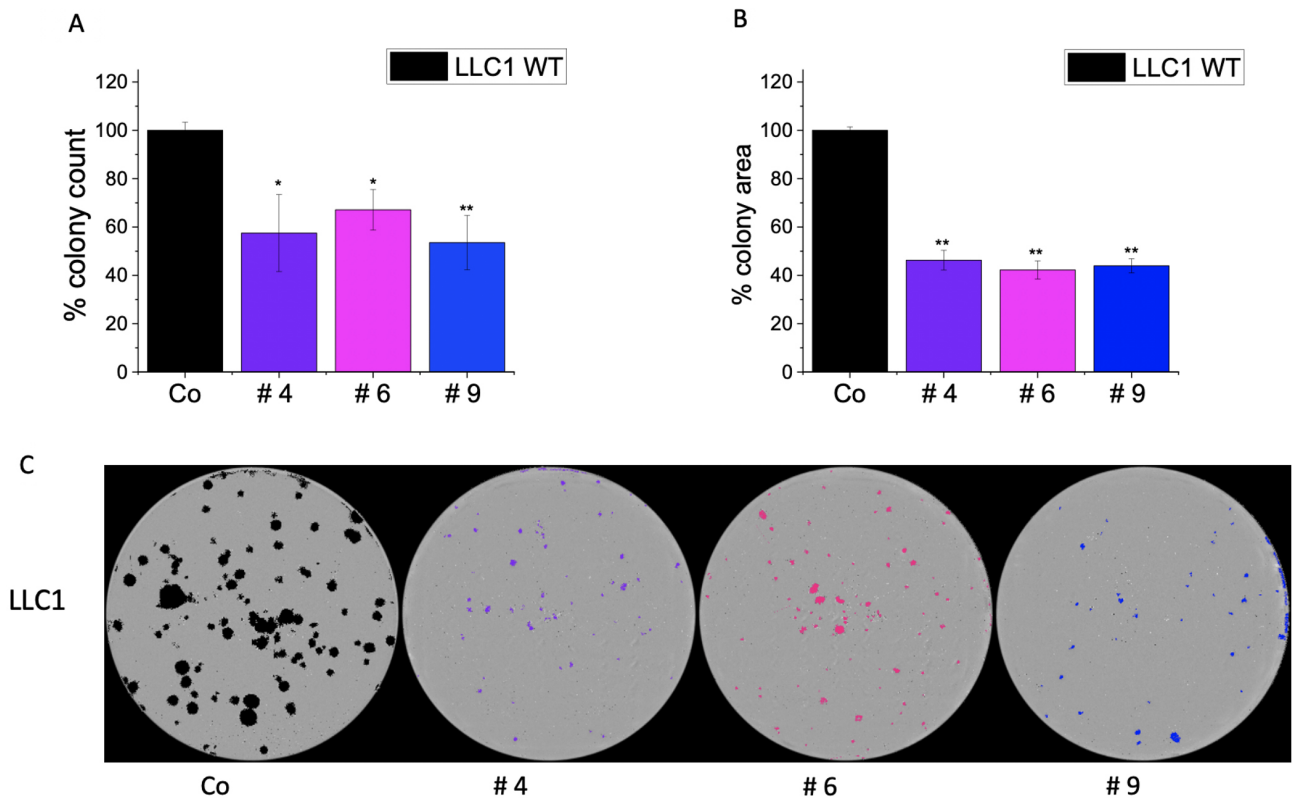
**Fig. 9. Effect of IMP2 inhibitors on wild-type LLC1 cells in colony formation assay.** Figures illustrate the (A) number of colonies, (B) average area of colonies, and (C) representative images of colonies seen in a 6-well plate. Colonies were counted, and the average area of colonies was determined using the IncuCyte® S3 live cell imaging system. A treatment concentration of 25 µM was applied for each compound. Data was normalized to untreated wild-type LLC1 cells/control (Co) and represented as mean ± SEM, n = 3, duplicates. *$p < 0.05$ and **$p < 0.01$ when compared to values of control cells.

**Table 4. $IC_{50}$ of IMP2 inhibitors in wild-type LLC1 cells.**

| Compound (#) | $IC_{50}$ |
|---|---|
| 4 | 25.23 µM |
| 6 | 23.90 µM |
| 9 | 28.45 µM |

$IC_{50}$, Inhibitory concentration 50.

regarding their migration ability (Fig. 11A). A significant reduction in cell migration was observed in the monoallelic IMP2 knockout clones Huh7, HepG2, and SW480 cells.

## 4. Discussion

Overexpression of *IGF2BP2* has been reported in several cancers, highlighting its prognostic role [2]. Previous studies have characterized the role of IMP2 as a tumor promoter in cancer through siRNA-mediated knockdown of *IGF2BP2* [9,13–15]. Our study aimed to generate IMP2 knockouts using CRISPR/Cas9-prime editing approaches to validate IMP2 as a potential anti-cancer target.

Previous research has used CRISPR/Cas9 to inactivate IMP2 and observed a decrease in 2D proliferation in var-ious cell lines, including Hep3B, HeLa, RD, HCC-1359, MB-231, and SNU-423, over 5 days. This was determined by assessing growth and cell numbers using a mixture of edited and non-edited cells [2]. These findings support our hypothesis that obtaining a single-cell derived IMP2 knockout is challenging in cancer cell lines, and thus, earlier studies have used a polyclonal mixture for analysis, which potentially only had a monoallelic gene deletion. In our study, we encountered difficulties in generating single-cell derived IMP2 biallelic knockouts in A549 and Huh7 cell lines despite successfully validating the sgRNAs used in the CRISPR/Cas9 system. This suggests that the absence of IMP2 may impair the ability of cells to form colonies and affect cancer cell proliferation.

Using our CRISPR/Cas9 approach, we successfully generated biallelic IMP2 knockouts in LLC1 cells. However, we were unable to achieve knockouts using the variant approach, prime editing. Our findings are consistent with previous observations that the prime editor 2 (PE2) system is challenging to use in the murine system [26]. Strategies that aim to reduce the size of the PE2 system have been proposed to improve the efficiency of prime editing [27–29].

Sanger sequencing confirmed that biallelic IMP2 knockout LLC1 cells exhibited reduced protein expression,
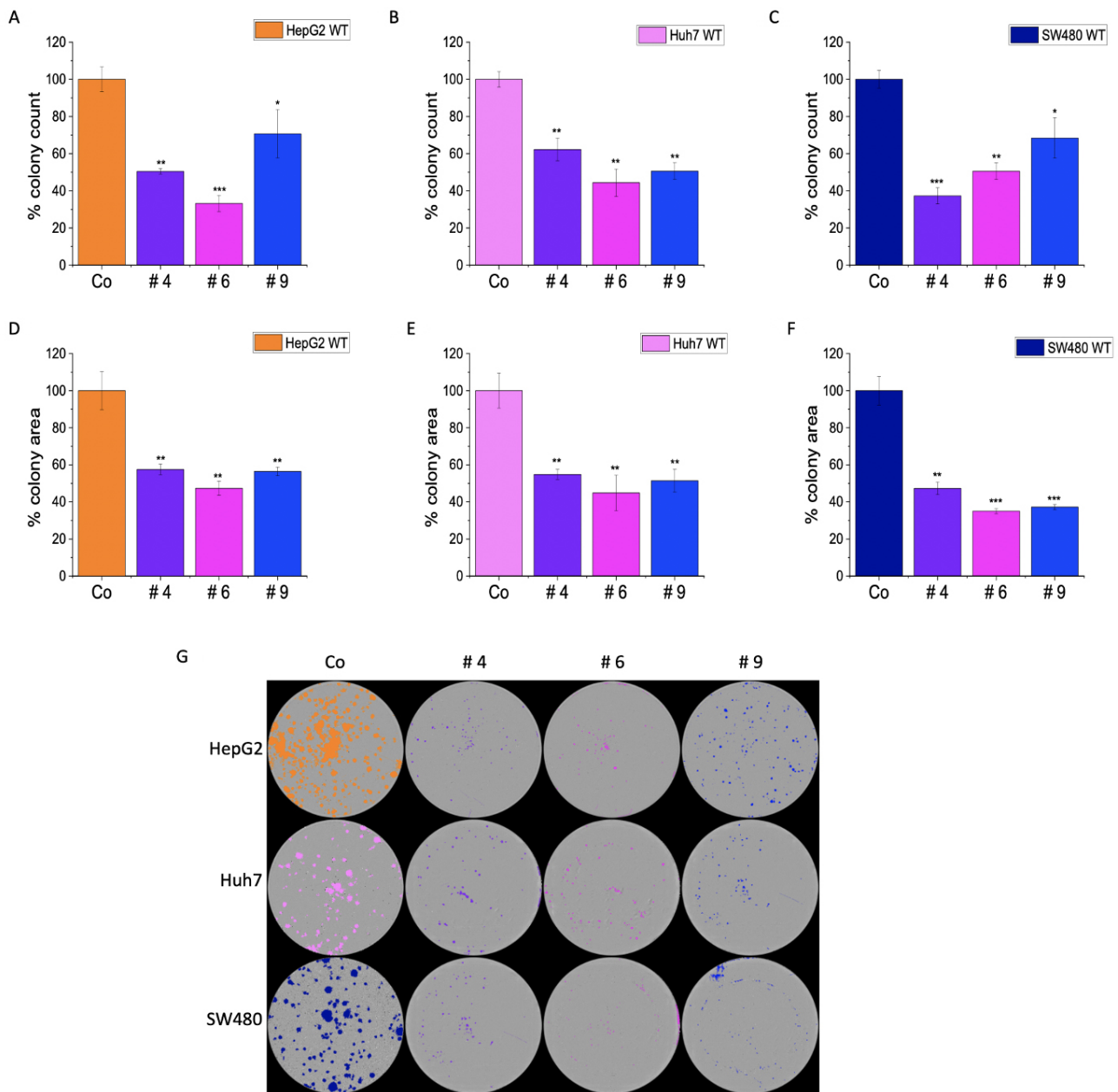
**Fig. 10. Effect of IMP2 inhibitors on Huh7, HepG2, and SW480 cells in colony formation assays.** Results present the number of colonies for (A) Huh7, (B) HepG2, and (C) SW480, as well as the average area of colonies for (D) Huh7, (E) HepG2, and (F) SW480 cells. Additionally, (G) representative images of colonies are shown as seen in a 6-well plate. The colonies were counted, and the average colony area was determined using a live cell imaging system, IncuCyte® S3. The Huh7, HepG2, and SW480 were monoallelic IMP2 knockouts. Data was normalized to untreated wild-type cells and represented as mean ± SEM, n = 2, triplicates. The treatment doses were as follows: For Huh7, comp 4: 35 μM, comp 6: 45 μM, and comp 9: 25 μM. For HepG2, comp 4: 30 μM, comp 6: 40 μM, and comp 9: 35 μM. For SW480, comp 4: 20 μM, comp 6: 50 μM, and comp 9: 35 μM. $*p < 0.05$, $**p < 0.01$, and $***p < 0.001$ when compared to values of respective wild-type (WT)/control (Co) cells.

ranging from 7% to 65%. Despite several attempts, we could not generate biallelically edited IMP2 knockouts in SW480, Huh7, and HepG2 cells, supporting the notion that IMP2 is crucial for cell proliferation [10]. These monoallelic IMP2 knockouts, verified by Sanger sequencing, also demonstrated protein expression levels of 40% to 80%, as previously reported [10]. While successful editing disrupted gene integrity in the IMP2 knockout clones, the genomic effects did not consistently result in reduced RNA levels or explain the protein abundance in the CRISPR-generated knockout cell lines [30].
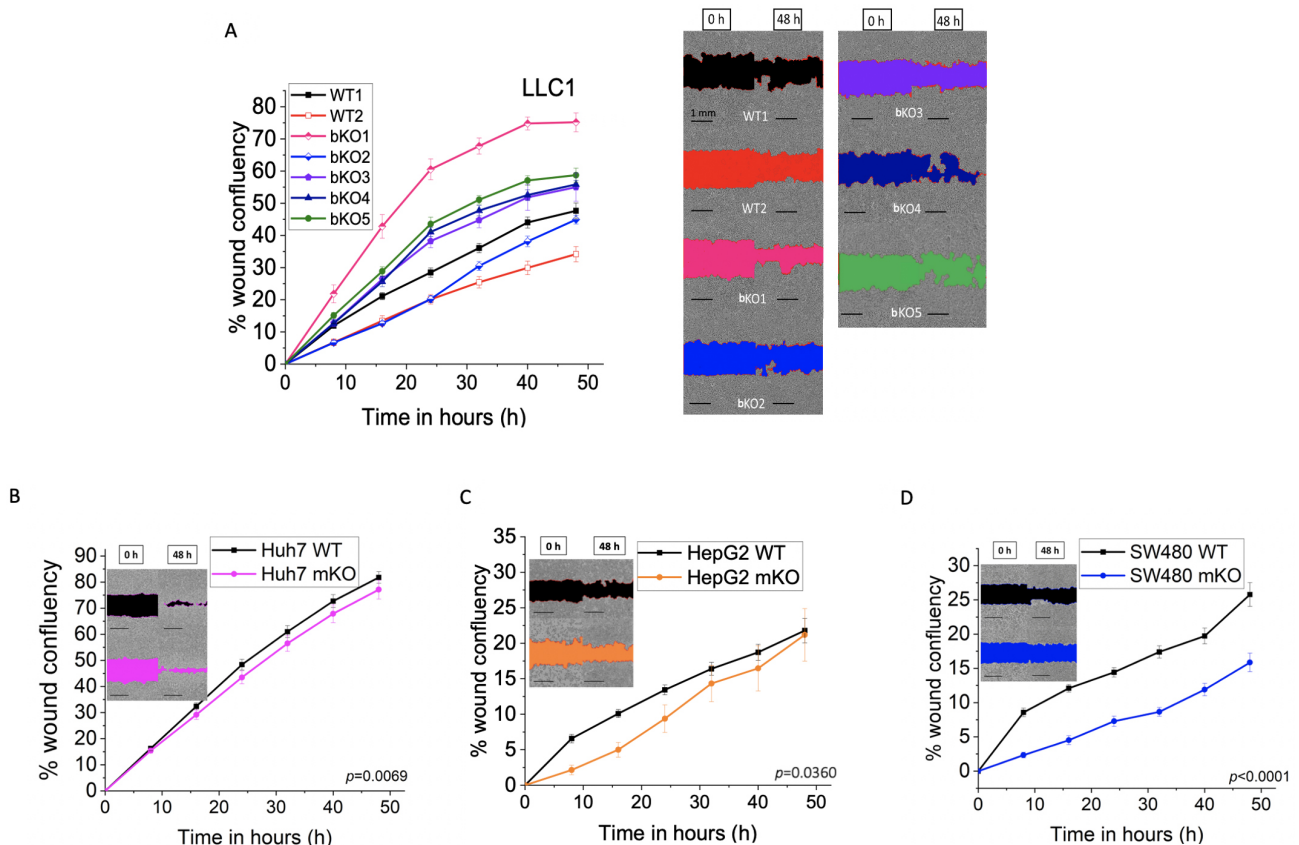
**Fig. 11. Effect of IMP2 knockout on cell migration in a wound healing assay.** (A) LLC1 (B) Huh7, (C) HepG2, and (D) SW480 cells were analyzed for cell migration using the IncuCyte® S3 system over a 48 h period. Representative pictures show the wound area in color at the starting point, 0 h, and 48 h after wounding, and the scale was set to 1 mm. The LLC1 wild-type clone is referred to as WT1, and the LLC1 editing control is referred to as WT2. The Huh7, HepG2, and SW480 were monoallelic IMP2 knockouts. Data are normalized to time point 0 h. Data is represented as mean ± SEM, n = 3 (quintuplicates). Panels (B–D) display *p*-values for WT vs. KO cells.

Other studies have investigated the impact of IMP2 knockdown using siRNA/shRNA-mediated approaches on colorectal carcinoma (CRC) cell lines. IMP2 knockdown exhibited reduced colony formation ability in HCT116 and SW480 [31], and also in SW620 and SW480 cells [5]. Similarly, IMP2 knockdown in SW480, SW620, and HCT-8 cells led to inhibition of 2D cell proliferation and reduced migration [9]. Our recent study focused on CRISPR/Cas9-prime mediated biallelic IMP2 knockout in HCT116 cells, which showed no effect on 2D proliferation but demonstrated reduced 3D proliferation, cell migration, and adhesion [10]. Recent research revealed that IMP2 is involved in the induction of chemoresistance in HCT116 [32]. Our data exhibited reduced proliferation at later time points, as well as decreased cell migration in CRISPR/Cas9-generated monoallelic IMP2 knockout SW480 cells.

Likewise, studies on hepatocellular carcinoma (HCC) cells have also demonstrated the impact of shRNA-mediated IMP2 knockdown. In HepG2 and Huh7 cells, IMP2 knockdown impeded cell proliferation and reduced clonogenicity [12]. Employing an siRNA knockdown of

p62, HepG2 cells showed no effect on 2D cell proliferation [6,7]. CRISPR/Cas9-mediated IMP2 knockout in HepG2 and SNU449 cells in a polyclonal mixture of transfected cells showed inconsistent effects on cell proliferation but reduced colony formation upon IMP2 inactivation [7]. Additionally, IMP2 inactivation in HepG2 cells reduced cell migration, while IMP2 overexpression in SNU449 cells promoted migration through epithelial-mesenchymal transition (EMT) induction *via* the Wnt/$\beta$-catenin pathway [7]. Tumor cells gain their migratory and invasive ability through EMT, eventually aiding in metastasis [33]. Similar effects on EMT induction were observed upon IMP2 overexpression in PANC-1 cells (pancreatic cancer) [33] and glioblastoma multiforme (malignant brain cancer) [34]. Our data on IMP2 knockout HCC cells showed reduced cell migratory ability. Our findings emphasize that IMP2 knockout results in reduced cell migratory ability, probably by hindering EMT. Moreover, our study confirmed reduced 2D proliferation in HepG2 IMP2 monoallelic knockout cells and clonogenicity in monoallelic IMP2 knockout HepG2 and Huh7 cells. The lack of effect observed on 2D prolif-

eration in Huh7 monoallelic IMP2 knockout could be attributed to the fact that the knockout clone still expresses nearly 80% of IMP2.

In non-small cell lung cancer cell lines A549 and H1975, sh-RNA-mediated IMP2 knockdown resulted in reduced proliferation and colony formation ability [3]. Our data showed no consistent effect on 2D proliferation but reduced colony formation in LLC1 biallelic IMP2 knockouts. In a study by Xu *et al.* [35], 2022, it was demonstrated that single-cell-derived cell lines (SCDCLs) from LLC1 cells display varying growth patterns. This discovery can help shed light on our findings regarding the proliferation of LLC1 cells. Specifically, our data indicate that bulk LLC1 cells (designated as WT1) exhibit slower growth than WT2, which have been derived from cells that underwent the CRISPR procedure without an edit of the IMP2 gene. Compared to this WT2 clone, three of the knockout clones grew slower (bKO1-3), while bKO4 grew faster. The action of IMP2 inhibitors on cell proliferation was reduced in four of the five knockout clones; this further supports an involvement of IMP2 in cell proliferation, but it is challenging to establish a clear trend due to the heterogeneous nature of the SCDCLs.

3D cell culture models provide valuable insights into tumor characteristics, such as proliferation, invasion, and metastatic potential [23]. The formation of MCTs relies on cell-cell adhesion molecules that initiate loose bonds between integrins and the extracellular matrix (ECM). The interaction through N-cadherin-to-E-cadherin plays a crucial role in the aggregation of cells into compact spheroids [23]. Previous studies have demonstrated a loss of spheroid-forming ability in colon cancer cells [36]. In our study, we investigated the effect of IMP2 knockout on the ability of HCC, CRC, and lung cancer cells to form spheroids. The knockout of IMP2 in all tested cell lines resulted in a loss of their ability to form compact spheroids. This can be attributed to a reduction in cell adhesion, as previously shown in biallelic edited IMP2 knockout HCT116 cells [10]. The role of IMP2 in spheroid formation in cancer has not been extensively studied before.

In our previous work, we examined the effects of newly identified IMP2 inhibitors on 2D cell proliferation in HCT116 and Huh7 cells and on 3D cell proliferation in HCT116 and SW480 cells [10]. These inhibitors showed inhibition of both 2D and 3D proliferation, which aligns with our findings of reduced 2D proliferation in LLC1 cells upon compound treatment. It is important to note that while the inhibition is not entirely specific to IMP2, the fact that the effect is more pronounced in wild-type cells compared to IMP2 knockout clones suggests a significant reliance on IMP2 inhibition [10]. In this work, we present novel findings indicating that these compounds also exert an effect on a mouse cancer cell line, i.e., LLC1. Interestingly, we observed a reduced sensitivity towards these compounds in biallelic IMP2 knockout LLC1 cells when compared to

their parental cell lines. It is worth mentioning that these compounds represent hits, which were identified through a screening approach [10] and have not been optimized for targeting IMP2 specifically. Nevertheless, the level of specificity we observed is quite noteworthy. Additionally, we observed reduced colony formation ability in LLC1, SW480, HepG2, and Huh7 cells following compound treatment.

## 5. Conclusions

In conclusion, our study validates IMP2 as a potential anti-cancer target in lung, liver, and colon cancer using *in vitro* models with the CRISPR/Cas9-prime editing-based gene knockout approach. This further supports the essential role of IMP2 in tumor cell proliferation, colony formation, and migration.

### Availability of Data and Materials

All data points generated or analyzed during this study are included in this article and there are no further underlying data necessary to reproduce the results.

### Author Contributions

AKK conceptualized and initiated the study. AKK, KL, CD, and SC designed the research study and reviewed the literature. SC, KL and JH performed the investigation and formal analysis. AKG helped analyze NGS results. HS analyzed the data on the effect of IMP2 inhibitors on 2D cell proliferation and metabolic activity in wild-type LLC1 cells. AKK contributed to the funding acquisition. ME and KW synthesized IMP2 inhibitors. SMK provided supporting data for the revision of the manuscript. SC wrote the original draft. SC, AKK, KL, JH, SMK, CD, KW, AKG, ME, and HS engaged in the review and editing of the manuscript. All authors read and approved the final manuscript. All authors have participated sufficiently in the work and agreed to be accountable for all aspects of the work.

### Ethics Approval and Consent to Participate

Not applicable.

## Funding

## Conflict of Interest

The authors declare no conflict of interest.

## Supplementary Material

Supplementary material associated with this article can be found, in the online version, at https://doi.org/10.31083/j.fbl2901041.

## References

[1] Mohibi S, Chen X, Zhang J. Cancer the 'RBP' eutics-RNA-binding proteins as therapeutic targets for cancer. Pharmacology & Therapeutics. 2019; 203: 107390.

[2] Dai N, Ji F, Wright J, Minichiello L, Sadreyev R, Avruch J. IGF2 mRNA binding protein-2 is a tumor promoter that drives cancer proliferation through its client mRNAs IGF2 and HMGA1. eLife. 2017; 6: e27155.

[3] Han L, Lei G, Chen Z, Zhang Y, Huang C, Chen W. IGF2BP2 regulates MALAT1 by serving as an N6-methyladenosine reader to promote NSCLC proliferation. Frontiers in Molecular Biosciences. 2022; 8: 780089.

[4] Shi R, Yu X, Wang Y, Sun J, Sun Q, Xia W, et al. Expression profile, clinical significance, and biological function of insulin-like growth factor 2 messenger RNA-binding proteins in non-small cell lung cancer. Tumour Biology: the Journal of the International Society for Oncodevelopmental Biology and Medicine. 2017; 39: 1010428317695928.

[5] Ye S, Song W, Xu X, Zhao X, Yang L. IGF2BP2 promotes colorectal cancer cell proliferation and survival through interfering with RAF-1 degradation by miR-195. FEBS Letters. 2016; 590: 1641–1650.

[6] Kessler SM, Pokorny J, Zimmer V, Laggai S, Lammert F, Bohle RM, et al. IGF2 mRNA binding protein p62/IMP2-2 in hepatocellular carcinoma: antiapoptotic action is independent of IGF2/PI3K signaling. American Journal of Physiology. Gastrointestinal and Liver Physiology. 2013; 304: G328–G336.

[7] Xing M, Li P, Wang X, Li J, Shi J, Qin J, et al. Overexpression of p62/IMP2 can promote cell migration in hepatocellular carcinoma via activation of the Wnt/$\beta$-catenin pathway. Cancers. 2019; 12: 7.

[8] Bigagli E, De Filippo C, Castagnini C, Toti S, Acquadro F, Giudici F, et al. DNA copy number alterations, gene expression changes and disease-free survival in patients with colorectal cancer: a 10 year follow-up. Cellular Oncology (Dordrecht). 2016; 39: 545–558.

[9] Cui J, Tian J, Wang W, He T, Li X, Gu C, et al. IGF2BP2 promotes the progression of colorectal cancer through a YAP-dependent mechanism. Cancer Science. 2021; 112: 4087–4099.

[10] Dahlem C, Abuhaliema A, Kessler SM, Kröhler T, Zoller BGE, Chanda S, et al. First small-molecule inhibitors targeting the RNA-binding protein IGF2BP2/IMP2 for cancer therapy. ACS Chemical Biology. 2022; 17: 361–375.

[11] Liu TY, Hu CC, Han CY, Mao SY, Zhang WX, Xu YM, et al. IGF2BP2 promotes colorectal cancer progression by upregulating the expression of TFRC and enhancing iron metabolism. Biology Direct. 2023; 18: 19.

[12] Pu J, Wang J, Qin Z, Wang A, Zhang Y, Wu X, et al. IGF2BP2 promotes liver cancer growth through an m6A-FEN1-dependent mechanism. Frontiers in Oncology. 2020; 10: 578816.

[13] Xu X, Yu Y, Zong K, Lv P, Gu Y. Up-regulation of IGF2BP2 by multiple mechanisms in pancreatic cancer promotes cancer proliferation by activating the PI3K/Akt signaling pathway. Journal of Experimental & Clinical Cancer Research: CR. 2019; 38: 497.

[14] Cao P, Wu Y, Sun D, Zhang W, Qiu J, Tang Z, et al. IGF2BP2 promotes pancreatic carcinoma progression by enhancing the stability of B3GNT6 mRNA via m6A methylation. Cancer Medicine. 2023; 12: 4405–4420.

[15] Dong L, Geng Z, Liu Z, Tao M, Pan M, Lu X. IGF2BP2 knockdown suppresses thyroid cancer progression by reducing the expression of long non-coding RNA HAGLR. Pathology, Research and Practice. 2021; 225: 153550.

[16] Boettcher M, McManus MT. Choosing the right tool for the job: RNAi, TALEN, or CRISPR. Molecular Cell. 2015; 58: 575–585.

[17] Uddin F, Rudin CM, Sen T. CRISPR gene therapy: Applications, limitations, and implications for the future. Frontiers in Oncology. 2020; 10: 1387.

[18] Giuliano CJ, Lin A, Girish V, Sheltzer JM. Generating single cell-derived knockout clones in mammalian cells with CRISPR/Cas9. Current Protocols in Molecular Biology. 2019; 128: e100.

[19] Anzalone AV, Randolph PB, Davis JR, Sousa AA, Koblan LW, Levy JM, et al. Search-and-replace genome editing without double-strand breaks or donor DNA. Nature. 2019; 576: 149–157.

[20] Dehairs J, Talebi A, Cherifi Y, Swinnen JV. CRISP-ID: decoding CRISPR mediated indels by Sanger sequencing. Scientific Reports. 2016; 6: 28973.

[21] Clement K, Rees H, Canver MC, Gehrke JM, Farouni R, Hsu JY, et al. CRISPResso2 provides accurate and rapid genome editing sequence analysis. Nature Biotechnology. 2019; 37: 224–226.

[22] Lu M, Nakamura RM, Dent ED, Zhang JY, Nielsen FC, Christiansen J, et al. Aberrant expression of fetal RNA-binding protein p62 in liver cancer and liver cirrhosis. The American Journal of Pathology. 2001; 159: 945–953.

[23] Han SJ, Kwon S, Kim KS. Challenges of applying multicellular tumor spheroids in preclinical phase. Cancer Cell International. 2021; 21: 152.

[24] Brix N, Samaga D, Hennel R, Gehr K, Zitzelsberger H, Lauber K. The clonogenic assay: robustness of plating efficiency-based analysis is strongly compromised by cellular cooperation. Radiation Oncology (London, England). 2020; 15: 248.

[25] Katz D, Ito E, Lau KS, Mocanu JD, Bastianutto C, Schimmer AD, et al. Increased efficiency for performing colony formation assays in 96-well plates: novel applications to combination therapies and high-throughput screening. BioTechniques. 2008; 44: ix–xiv.

[26] Aida T, Wilde JJ, Yang L, Hou Y, Li M, Xu D, et al. Prime editing primarily induces undesired outcomes in mice. BioRxiv. 2020; 2020-08

[27] Böck D, Rothgangl T, Villiger L, Schmidheini L, Matsushita M, Mathis N, et al. In vivo prime editing of a metabolic liver disease in mice. Science Translational Medicine. 2022; 14: eabl9238.

[28] Liu P, Liang SQ, Zheng C, Mintzer E, Zhao YG, Ponnienselvan K, et al. Improved prime editors enable pathogenic allele correction and cancer modelling in adult mice. Nature Communications. 2021; 12: 2121.

[29] Zheng C, Liang SQ, Liu B, Liu P, Kwan SY, Wolfe SA, et al. A flexible split prime editor using truncated reverse transcriptase improves dual-AAV delivery in mouse liver. Molecular Therapy: the Journal of the American Society of Gene Therapy. 2022; 30: 1343–1351.

[30] Smits AH, Ziebell F, Joberty G, Zinn N, Mueller WF, Clauder-Münster S, et al. Biological plasticity rescues target activity in CRISPR knock outs. Nature Methods. 2019; 16: 1087–1093.

[31] Liu T, Han C, Hu C, Mao S, Sun Y, Yang S, *et al*. Knockdown of IGF2BP2 inhibits colorectal cancer cell proliferation, migration and promotes tumor immunity by down-regulating MYC expression. Xi Bao Yu Fen Zi Mian Yi Xue Za Zhi = Chinese Journal of Cellular and Molecular Immunology. 2023; 39: 303–310. (In Chinese)

[32] Kendzia S, Franke S, Kröhler T, Golob-Schwarzl N, Schweiger C, Toeglhofer AM, *et al*. A combined computational and functional approach identifies IGF2BP2 as a driver of chemoresistance in a wide array of pre-clinical models of colorectal cancer. Molecular Cancer. 2023; 22: 89.

[33] Dahlem C, Barghash A, Puchas P, Haybaeck J, Kessler SM. The insulin-like growth factor 2 mRNA binding protein IMP2/IGF2BP2 is overexpressed and correlates with poor survival in pancreatic cancer. International Journal of Molecular Sciences. 2019; 20: 3204.

[34] Mu Q, Wang L, Yu F, Gao H, Lei T, Li P, *et al*. Imp2 regulates GBM progression by activating IGF2/PI3K/Akt pathway. Cancer Biology & Therapy. 2015; 16: 623–633.

[35] Xu BL, Wang XM, Chen GY, Yuan P, Han L, Qin P, *et al*. *In vivo* growth of subclones derived from Lewis lung carcinoma is determined by the tumor microenvironment. American Journal of Cancer Research. 2022; 12: 5255–5270.

[36] Stadler M, Scherzer M, Walter S, Holzner S, Pudelko K, Riedl A, *et al*. Exclusion from spheroid formation identifies loss of essential cell-cell adhesion molecules in colon cancer cells. Scientific Reports. 2018; 8: 1151.